The *Chlamydomonas* Kinesin-like Protein FLA10 Is Involved in Motility Associated with the Flagellar Membrane

Keith G. Kozminski, Peter L. Beech, and Joel L. Rosenbaum

Department of Biology, Yale University, New Haven, Connecticut 06511

Abstract. The *Chlamydomonas FLA10* gene was shown to encode a flagellar kinesin-like protein (Walther, Z., M. Vashishtha, and J. L. Hall. 1994. *J. Cell Biol.* 126:175–188). By using a temperature-sensitive allele of *FLA10*, we have determined that the FLA10 protein is necessary for both the bidirectional movement of polystyrene beads on the flagellar membrane and intraflagellar transport (IFT), the bidirectional movement of granule-like particles beneath the flagellar membrane (Kozminski, K. G., K. A. Johnson, P. Forscher, and J. L. Rosenbaum. 1993. *Proc. Natl. Acad. Sci. (USA).* 90:5519–5523). In addition, we have correlated the presence and position of the IFT particles visualized by light microscopy with that of the electron dense complexes (rafts) observed beneath the flagellar membrane by electron microscopy. A role for FLA10 in submembranous or flagellar surface motility is also strongly supported by the immunolocalization of FLA10 to the region between the axonemal outer doublet microtubules and the flagellar membrane.

THE eukaryotic flagellum exhibits motilities that are independent of dynein-based flagellar beating (reviewed in Bloodgood, 1990; Bloodgood, 1992). These beat-independent motilities are associated with the flagellar membrane and include the gliding of cells over solid substrata by means of their flagella (Lewin, 1952; Bloodgood, 1981; Kozminski et al., 1995) and the bidirectional movement of polystyrene beads on the flagellar surface (Bloodgood, 1977; Kozminski et al., 1995). In the unicellular biflagellate green alga *Chlamydomonas*, we recently described another beat-independent flagellar motility, termed intraflagellar transport (IFT)[1]. This motility occurs beneath the flagellar membrane and involves the bidirectional movement of granule-like particles along the length of the flagellum (Kozminski et al., 1993*b*, 1995). We suggested (Kozminski et al., 1993*b*) that the moving IFT particles visualized by video-enhanced differential-interference contrast (DIC) microscopy (see Fig. 1 *a*, *arrows*) were the large electron-dense complexes or "rafts" observed beneath the flagellar membrane by electron microscopy (see Fig. 1, *b–d*; see also Ringo, 1967; Mesland et al., 1980; Kozminski et al., 1993*b*). Although the relationship of the rafts to the IFT particles has remained an important question, we first sought to identify the molecular motor(s) driving these motilities.

Address correspondence to Joel L. Rosenbaum, PO Box 208103, Yale University, New Haven, CT 06520-8103.

1. *Abbreviations used in this paper*: DIC, differential interference-contrast; IBMX, 3-isobutyl-1-methyl-xanthine; IFT, intraflagellar transport; M_I, minimal medium.

Initial studies aimed at identifying the motors driving gliding, bead movement, and IFT revealed multiple kinesin-like proteins (klps) within the flagella of *Chlamydomonas* (Fox et al., 1992; Kozminski et al., 1992; Kozminski, 1995*a*). Individual klps were subsequently localized by immunochemical methods to specific subsets of flagellar microtubules (reviewed in Bernstein and Rosenbaum, 1994). Among the nine outer doublet and two central pair microtubules of the flagellar axoneme, two klps were localized by immunoelectron microscopy to the central pair microtubules, though it was not clear if both klps were on the same microtubule (Bernstein et al., 1994; Johnson et al., 1994). The presence of a third central pair-associated klp was detected in an immunoblot analysis of wild-type flagella and mutant flagella lacking the central pair apparatus (Fox et al., 1994; Johnson et al., 1994). This analysis further suggested that an additional flagellar klp was associated with the outer doublet microtubules. The putative outer doublet-associated klp, initially identified immunochemically, also had the biochemical properties of kinesin, such as an ATP-dependent release from axonemal and brain microtubules (Fox et al., 1994). In comparison to the central pair-associated klps, the proximity of this klp to the flagellar membrane made it the best candidate among the flagellar klps for a motor involved in bead movement and IFT (Fox et al., 1994).

Concurrent with the studies just described, Walther et al. (1994) cloned the *Chlamydomonas FLA10* gene and showed that it encoded a flagellar klp. The *FLA10* locus was first identified in screens for mutants that failed to regenerate or maintain stable flagella at 32°C (Huang et al., 1977; Adams et al., 1982). More than a dozen tempera-

© The Rockefeller University Press, 0021-9525/95/12/1517/11 $2.00

ture-sensitive *fla10* alleles have been identified (Dutcher, 1989), with each allele displaying its own unique kinetics of flagellar instability (i.e., flagellar shortening) at the restrictive temperature (Dutcher, 1989; Lux and Dutcher, 1991). Because preliminary data suggested that IFT is essential for flagellar integrity (Kozminski, 1995*a*), we investigated the possibility that the flagellar klp encoded by the *FLA10* locus (Walther et al., 1994), FLA10, is involved in one or more of the beat-independent flagellar motilities.[2] By use of temperature-shift experiments and high-resolution video-enhanced DIC microscopy, we have determined that FLA10 is required for two motilities, IFT and bead movement. With a FLA10-specific antibody, we have also determined that FLA10 is the klp that was first identified (see above) as being associated with the outer doublet microtubules (Fox et al., 1994; Johnson et al., 1994) and have shown directly, by immunogold electron microscopy, that FLA10 is localized between the outer doublet microtubules and the flagellar membrane. These data represent the first localization of a flagellar klp to the region between the axonemal outer doublet microtubules and the flagellar membrane, the exact site where one would expect to find a motor involved with submembranous or flagellar surface motility.

Materials and Methods

Cultures

Chlamydomonas moewusii strain *M475* (CC957) and *C. reinhardtii* strains *21gr* (CC1690), *pf1* (CC1024), and *fla10-1* (CC1919) were obtained from the *Chlamydomonas* Genetics Center (Duke University, Durham, NC). The strain *fla10-1* was originally designated dd-a-224 and is temperature-sensitive due to a single genetic lesion (Huang et al., 1977). Log-phase, synchronously dividing cultures were grown in minimal medium (M_I) (Sager and Granick, 1953) at 22–23°C on a 14:10 h light/dark cycle with continuous aeration.

Crosses

To facilitate the observation of flagella by light microscopy, *fla10-1* was crossed into a *pf1* background. *pf1* cells, which are deficient in radial spoke protein 4 and thus the radial spoke head, have flaccid, paralyzed flagella (Luck et al., 1977; Piperno et al., 1977; Huang, 1986; Curry et al., 1992) that are amenable to video analysis (Kozminski, 1995*b*). Gametes were made from synchronized, vegetative M_I cultures and mated as previously described (James, 1989). Phase-contrast microscopy was used to screen the progeny of dissected tetrads for immotile (paralyzed-flagella) cells in synchronous M_I cultures. To identify progeny bearing the temperature-sensitive *fla10-1* allele, aliquots of synchronously-growing cells were placed in test tubes and incubated for 4 h at 20°C and 32°C; the cells were then examined by phase microscopy for the presence of flagella. *pf1 fla10-1* double mutants retained their flagella at 20°C, but like the parental *fla10-1* strain, not at 32°C.

Flagellar Resorption

To induce flagellar resorption at the permissive temperature, cells were pelleted, washed with low calcium/high sodium M_I medium (no $CaCl_2$, 25 mM sodium citrate), repelleted, and then resuspended once again in low calcium/high sodium M_I medium (Lefebvre et al., 1978). In an alternative method, cells were pelleted, washed with M_I medium, repelleted, and then resuspended in M_I medium containing 0.5 mM 3-isobutyl-1-methyl-xanthine (IBMX; Sigma, St. Louis, MO) (Lefebvre et al., 1980). With *fla* mutants, flagellar resorption was also induced by shifting the cultures from the permissive (20°C) to restrictive temperature (32°C) (Huang et al., 1977; Adams et al., 1982; Lux and Dutcher, 1991).

Flagellar Length Measurements

To measure flagellar length in time course experiments that did not involve flagellar isolation, cells were pelleted and then resuspended to a final concentration of 1–2 × 10^6 cells/ml in M_I medium or treated as described above to induce flagellar resorption. The cells were transferred to glass test tubes and gently agitated at 50 rpm under continuous light at either 20°C or 32°C in an AquaTherm water bath shaker (New Brunswick Scientific, New Brunswick, NJ). Aliquots were removed and fixed with Lugol's solution (6% KI, 4% iodine in water). 30–50 flagella per sample were measured on a Zeiss phase-contrast microscope calibrated with a stage micrometer.

Quantitation of Flagellar Surface Motility

To quantify flagellar surface motility, log-phase cultures, grown synchronously in M_I medium, were centrifuged for 5–10 min at 1,500 rpm in an IEC centrifuge. The cell pellets were resuspended to a final concentration of 3.5 × 10^6 cells/ml in fresh M_I media or treated as described above to induce flagellar resorption. 40 μl of cells were mixed with either 120 μl M_I medium, M_I medium with 0.5 mM IBMX, or low calcium/high sodium M_I medium, and 40 μl of a 1:100 dilution of polystyrene beads each prewarmed to either 20 or 32°C. The polystyrene beads (0.3-μm diam; Polysciences, Inc., Warrington, PA) were prepared by washing four times with double distilled water (Bloodgood, 1995). Bead movement on the flagellar surface was immediately scored using a phase-contrast microscope. The number of flagella examined, number of beads bound, and number of beads moving were recorded over a period of 3 min.

Video Microscopy

In preparation for video microscopy, cells were resuspended in fresh M_I medium and placed between two No. 1 coverslips (Corning Inc., Corning, NY) supported with 0.5-mm plastic shims; Vaseline was used to seal the chamber. A Zeiss Axiovert microscope fitted with DIC optics was used for all experiments. The preparation of coverslip chambers, optics, and method of digital data acquisition have been detailed previously (Kozminski et al., 1993*b*; Kozminski, 1995*b*). For temperature-shift experiments, the cells were heated to the permissive temperature (20°C) or restrictive temperature (32°C) within the coverslip chamber. Heat was transferred to the chamber by warming both the condenser and objective with Kapton heaters, 0.5 × 4 in, 5W, 28V and 1 × 3 in, 7.5W, 28V, respectively (Electroflex Heat Inc., Bloomfield, CT); the chamber temperature was controlled by manually adjusting the current through the heaters. To measure the internal temperature of the chamber to ± 0.1°C, a 0.009-in Type T Tissue Implant Probe (Cole-Parmer, Niles, IL) connected to a Digi-Sense thermocouple thermometer (Cole-Parmer, Niles, IL) was inserted into the chamber.

Electron Microscopy

For the analysis of rafts between the flagellar membrane and axoneme, vegetative cells were pelleted and resuspended to a concentration of 3.5 × 10^6 cells/ml in 10 mM Hepes-KOH, pH 7.4. The cells were either left untreated or induced to resorb their flagella as described above. Cells were fixed, processed, and embedded as previously described (Kozminski et al., 1993*b*), but were not included in a block of low melting temperature agarose after fixation. Addition of 0.8% $K_3Fe(CN)_6$ to the postfixation step greatly enhanced the ability to visualize rafts. Silver/gold thin sections were cut with a diamond knife, stained with 2% (wt/vol) uranyl acetate for 30 min, washed 4 times with double distilled water, stained with Reynolds' lead citrate (Reynolds, 1963) for 4 min, and washed 4 times with double distilled water. Thin sections were examined on a Zeiss EM10 transmission electron microscope. For determining the number of rafts between the flagellar membrane and axoneme, control and experimental grids were scored blind. Rafts were scored only in transverse sections of flagella.

Single Cell Light and Electron Microscopy

Cells were fixed and embedded as described above; however, before poly-

2. The *FLA10* gene product was originally named KHP1 for kinesin-homologous protein 1 (Walther et al., 1994). For consistency with the newly adopted standard of genetic nomenclature for *Chlamydomonas* (Dutcher, 1995), we suggest that FLA10 be used to represent the *FLA10* gene product.

merization of the resin, cells were sandwiched between two teflon-coated glass microscope slides (Fluoroglide CP, Electron Microscopy Sciences, Ft. Washington, PA). After polymerization, the slides were separated with a razor blade. A thin wafer of resin (~0.5 mm thick) was peeled from the slides and affixed at its corners to an acid-washed No. 1 coverslip with Duro SuperGlue (Loctite Corporation, Cleveland, OH); the flat-embedded cells were observed by video-enhanced DIC microscopy. The optics and methods of digital data acquisition and image enhancement have been detailed previously (Kozminski et al., 1993*b*; Kozminski, 1995*b*). The relative position of the cell of interest was diagrammed, and a resin chip containing the cell was excised and mounted on a block for thin-sectioning. Serial sections through the flagellar region were collected, stained, and observed as described above. To spatially correlate IFT particles and rafts, electron and light micrographs were enlarged to equivalent sizes using the flagellar tip and the apical papillum of the cell as reference points. Rafts were marked on acetate overlay tracings that were compiled from electron micrographs of the complete series of flagellar sections. Some error would be expected in this process, primarily from differential section shrinkage. However, the fact that the IFT particles visible in the light microscope align with rafts to within less than 0.25 μm makes us confident that the observed correlation is accurate.

Flagellar Isolation and Fractionation

Two standard methods of flagellar isolation and fractionation were employed with modification. For the STEEP + Ca^{2+} method (Witman et al., 1972), 8 l of cells were concentrated by centrifugation. After deflagellation, deflagellated cells and flagella were added to 250-ml conical bottles and underlaid with 50–75 ml of 25% sucrose (wt/vol) in STEEP (0.15 M sucrose, 15 mM Tris-Cl, pH 7.8, 2.5 mM EDTA, pH 7.8, 11% (vol/vol) ethanol, and 30 mM KCl) and 15 mM $CaCl_2$. Cells bodies were removed by centrifuging for 10 min at 1,600 rpm at 0°C in an IEC 259 rotor (no brake). The suspension of flagella above the cushion was collected and the flagella were pelleted for 20 min at 10,000 rpm at 4°C in a Sorvall SS-34 rotor. Flagellar pellets were resuspended in 5-6 ml HMDEK (10 mM Hepes-KOH, pH 7.2, 5 mM $MgSO_4$, 1 mM DTT, 0.5 mM EDTA, pH 7.2, 25 mM KCl), transferred to 12-ml conical Pyrex tubes, and underlaid with an equal volume of 25% sucrose (wt/vol) in HMDEK. Any cell bodies remaining in the preparation were removed by centrifuging for 10 min at 4°C at 1,500 rpm in an IEC centrifuge. The suspension of flagella above the cushion was collected and the flagella pelleted for 10 min at 4°C at 8,000 rpm in a Sorvall HB-4 rotor. Flagellar pellets were resuspended in HMDEK containing 1 mM PMSF, 5 μg/ml pepstatin A, 20 μM taxol to stabilize the central pair microtubules, and 1% NP-40 to solubilize the flagellar membrane. Axonemes were pelleted for 10 min at 4°C at 8,000 rpm in a microfuge. The supernatant containing the detergent soluble membrane + matrix fraction was collected and the axonemes were resuspended in HMDEK with PMSF, pepstatin A, and 10 μM taxol. The axonemes were pelleted as before and washed in HMDEK with PMSF and pepstatin A.

A modified version of the pH-shock method (Witman et al., 1972) was used to isolate flagella during time course experiments at 32°C. Cells from 16 l of synchronous M_1 culture were concentrated with a Pellicon filtration system (Witman, 1986) and then pelleted. The cell pellets were resuspended in 5% sucrose (wt/vol) in 10 mM Hepes-KOH, pH 7.4, to a final concentration of ~10^7 cells/ml (600 ml). 400–600-ml aliquots were transferred to 1 l Erlenmyer flasks (time 0), one flask for each time point, and warmed to 32°C in an AquaTherm water bath shaker (New Brunswick Scientific, New Brunswick, NJ) shaking at 50 rpm. After the culture medium reached 32°C (15 min), deflagellation by pH shock was performed, at given time points, directly in each flask without further concentration of the cells. Cell bodies were removed by pelleting through two 25% (wt/vol) sucrose in HMDEK cushions as described above for the STEEP + Ca^{2+} procedure. As a control, flagella were also isolated at 21–23°C.

SDS-PAGE and Immunoblots

Flagellar proteins were separated on 4–14% mini-polyacrylamide gradient gels with 0.1% SDS (Baker, Phillipsburg, NJ) according to the method of Laemmli (1970). The protein concentration of isolated flagella was determined by a Bradford protein assay (Bio-Rad, Hercules, CA) using a BSA standard. Immunoblots were performed as previously described (Kozminski et al., 1993*a*). Blots were incubated with primary antibodies overnight at 4°C at the following dilutions: *Volvox* actin A5 antibody, 1:2,000; FLA10 antibody, 1:500; LAGSE antibody and Klp1 tail antibody, 1:5,000.

Cloning of the FLA10 Tail Region

First strand synthesis for reverse transcription PCR was performed on 3.0 μg of poly(A)$^+$ mRNA isolated from *Chlamydomonas* cells 40 min into flagellar regeneration (Bernstein et al., 1994) and primed with the *FLA10* anti-sense oligonucleotide TTGACCGAGTCGCGCAGTGAGC (nucleotides 2258–2237, Walther et al., 1994) at 16 μg/ml. The RNA/primer mixture was heated to 70°C (10 min) and chilled on ice followed by the addition of AMV reverse transcriptase (25 units; Boehringer Mannheim, Indianapolis, IN) and dNTPs (1 mM final) to a total volume of 20 μl; reverse transcription was performed at 42°C for 40 min. The resultant cDNA was used for PCR amplification as described (Bernstein et al., 1994). First round PCR was primed with CGATGTCGGTGATGTCCTTGCC (*FLA10* anti-sense nucleotides 2236–2215) and GATGCTTCGCCAGTTCCAGGAG (*FLA10* sense nucleotides 1098–1119). A product of the predicted size was synthesized, gel purified, and primed with GCAATTCTTGAGCCGCTCG (*FLA10* anti-sense nucleotides 2064–2046) and GACATCGACGCCATCAAGG (*FLA10* sense nucleotides 1246–1264) for a second round of PCR. The final PCR product (an 819-bp fragment 1246–2064) was gel purified, treated with T4 DNA polymerase and T4 polynucleotide kinase (New England Biolabs, Beverly, MA), and subcloned into the EcoRV site of pBluescript II KS(+) (Stratagene, San Diego, CA). Individual clones were isolated and sequenced; the clone chosen for further work differed from *FLA10* (Walther et al., 1994) by a single, silent mutation (an A to G transition) at position 1518. The cloned fragment was then excised using the BamHI and HindIII sites of pBluescript and inserted into the corresponding sites of the His_6 fusion vector pQE30 (QIAGEN Inc., Chatsworth, CA).

Antibodies

FLA10 antibody was raised against amino acids 416–688 of the unique COOH-terminal tail region of FLA10, which was expressed in *E. coli* as a His_6-FLA10 fusion protein (above). Recombinant protein was purified from *E. coli* strain XL1 Blue as described (Bernstein et al., 1994). Polyacrylamide gel slices containing the 35-kD recombinant protein were used to immunize two rabbits; immunizations and bleeds were performed as previously described (Bernstein et al., 1994) by Yale Veterinary Services, except that 50 μg of protein was used for the first two immunizations and 25 μg for subsequent boosts. Affinity purification of the FLA10 antibody was performed on nitrocellulose strips according to the method of Olmsted (1981) as modified by Snyder (1989).

Affinity-purified polyclonal LAGSE antibody (L1) (Sawin et al., 1992) was the gift of K. Sawin and T. Mitchison (University of California, San Francisco, CA). Polyclonal antibody A5 against an NH_2-terminal decapeptide of *Volvox* actin was the gift of D. Kirk (Washington University, St. Louis, MO) and Rüdiger Schmitt (University of Regensburg). Affinity-purified polyclonal *Chlamydomonas* KLP1 tail antibody was described previously (Bernstein et al., 1994).

Immunoelectron Microscopy

For postembedding immunolocalization, wild-type *21gr* cells were fixed in 0.75% glutaraldehyde in 20 mM Pipes (pH 7.1) on ice for 30–40 min. A loose pellet of fixed cells was washed in buffer, dehydrated to 80% ethanol, and embedded in LR Gold (London Resin Company, Hampshire, UK) at −20°C for 36 h. The LR Gold was polymerized at −20°C under white fluorescent light with 0.2% (wt/vol) benzil as the catalyst. Silver/gold thin-sections were collected on colloidin or formvar-coated nickel grids, blocked and immunolabeled as previously described (Bernstein et al., 1994). Affinity-purified LAGSE antibody was used at a 1:1,000 dilution and affinity-purified FLA10 antibody was used at a 1:100 dilution; the primary antibodies were detected with 12-nm colloidal gold conjugated to goat anti-rabbit IgG (Jackson Immunologicals, West Grove, PA). Labeled sections were stained with 2% aqueous uranyl acetate for 5 min, rinsed for 10 s with distilled water, and wicked dry.

Results

Cessation of Beat-independent Flagellar Motilities in fla10 Cells at 32°C

To determine whether the flagellar kinesin-like protein

(klp), FLA10, is involved in a beat-independent flagellar motility, we examined the temperature-sensitive *Chlamydomonas fla10-1* (hereafter called *fla10*) mutant by video-enhanced DIC microscopy. The motility of particular interest was IFT, a beat-independent flagellar motility that we recently described in *Chlamydomonas* as the bidirectional movement of particle-like material beneath the flagellar membrane (Kozminski et al., 1993*b*). It was suggested (Kozminski et al., 1993*b*; Fox et al., 1994; Walther et al., 1994) that IFT (Fig. 1 *a*) is driven by a flagellar klp, in at least one direction, along the length of the flagellum. To facilitate the observation of flagella in *fla10* cells, the motile *fla10* mutant was crossed with the paralyzed-flagella mutant *pf1*.

At the permissive temperature (20°C), both *pf1* cells and the *pf1 fla10* double mutant exhibited IFT and polystyrene bead movement on the flagellar surface (Table I). The

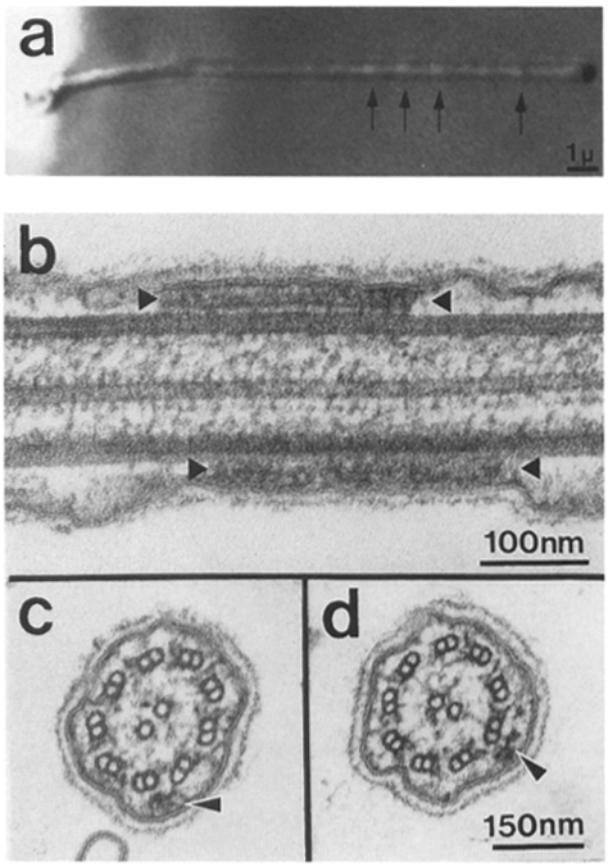

Figure 1. (*a*) Digital video-enhanced DIC image showing IFT. Granule-like particles, which move bidirectionally along the length of the flagellum, can be observed as regions of high contrast (*arrows*). The particles move to the flagellar tip at 2 μm/s or to the flagellar base at 3.5 μm/s, on average, without stopping or reversing direction (Kozminski et al., 1993*b*). The highly refractive cell body is located to the left. Reprinted with permission from Kozminski et al. (1993*b*). (*b*) EM longitudinal section of a *pf1* flagellum showing two electron dense complexes or rafts between the outer doublet microtubules and the flagellar membrane. Each raft (between arrow heads) is distinct from the flagellar membrane and is composed of a variable number of non-vesicular, lollipop-shaped structures. (*c* and *d*) EM transverse sections of a *pf1* flagellum and *fla10* flagellum, respectively. Arrowheads indicate rafts.

submembranous particles characteristic of IFT moved bidirectionally along the flagella of both *pf1* and *pf1 fla10* cells at similar rates (data not shown). IFT was more difficult to visualize, however, in the double mutant because fewer particles were observed moving in the flagella of *pf1 fla10* cells as compared to *pf1* cells. The reduced number of IFT particles observed in the flagella of *pf1 fla10* cells at 20°C was consistent with the report that cells bearing *fla10* alleles can display partial nonconditional mutant phenotypes (Lux and Dutcher, 1991). Motility on the flagellar surface was also very similar between *pf1* and *pf1 fla10* cells at 20°C (Table I). 45 and 50% of the polystyrene beads that bound to the flagellar surface of *pf1* and *pf1 fla10* cells, respectively, were observed moving along the length of the flagellum. The rate of bead movement and the percentage of beads moving approximated that reported for other *Chlamydomonas* strains (Bloodgood, 1977; Bloodgood et al., 1979; Kozminski et al., 1993*b*).

When *pf1 fla10* cells were shifted from the permissive temperature (20°C) to the restrictive temperature (32°C), both IFT and bead movement ceased completely within 60–90 min (Table I), although bead adhesion to the flagellar membrane was not affected. The first notable loss of IFT in *pf1 fla10* cells was evident by 30 min at 32°C (data not shown), which is the same period of time when *fla10* cells lose the ability to assemble new flagella at 32°C if experimentally deflagellated (Huang et al., 1977), suggesting that IFT is required for flagellar assembly. With *pf1* control cells, IFT, bead movement, and gliding motility continued normally at the restrictive temperature (Table I). Gliding motility in the *pf1 fla10* cells could not be assessed, however, because these cells adhered poorly to coverslips at both 20 and 32°C. With the *pf1 fla10* cells at 32°C, the loss of IFT and bead movement in both directions was gradual, concomitant, and equal along the length of the flagella. The cessation of IFT was observed specifically as a decrease in the number of particles moving along the length of the flagella, rather than as a decrease in the rates of particle movement. After the complete cessation of IFT (60–90 min at 32°C), only a minimal recovery of IFT was observed when *pf1 fla10* cells were shifted down to the permissive temperature for 3–4 h.

Depending upon the allele, the flagella of *fla10* cells resorb asynchronously and completely within 5–24 h after the shift from 20 to 32°C, with the onset of flagellar resorption either being immediate upon temperature shift or delayed several hours (Huang et al., 1977; Adams et al., 1982; Dutcher, 1989; Lux and Dutcher, 1991; this study). As expected for cells bearing the *fla 10-1* allele at 32°C (Huang et al., 1977; Dutcher, 1989; Walther et al., 1994), flagellar resorption began after a lag of ~60 min (see Fig. 4 *a* and data not shown). In the *pf1 fla10* double mutant, however, the initiation of flagellar resorption began immediately upon shifting to 32°C (see Fig. 4 *a* and data not shown). This premature temperature-induced flagellar shortening in the double mutant was not unexpected because *pf1* cells in minimal medium have also been shown to immediately undergo temperature-induced flagellar resorption, albeit at a substantially slower rate than *fla10-1* cells (Jarvik and Rosenbaum, 1980). When the flagella of *pf1 fla10* cells were induced to resorb with IBMX at 20°C (Lefebvre et al., 1978), bead movement and IFT continued normally

Table I. Video-Enhanced DIC & Phase-contrast Microscopy Observations of fla10 Cells

Cell Line	Condition	IFT		Bead movement		Flagellar length	
		0 min	90 min	0 min	90 min	0 min	90 min
				moving/total bound × 100		*mean in μm‡*	
pf1	20°C	+++	+++	45	70	9.2	8.1
	32°C		+++		60		6.5
	Low Ca^{2+}/high Na^+, 20°C		+++		0		4.5
pf1 fla10	20°C	++	++	50	48	8.5	8.4
	32°C		−−		0		4.2
	0.5 mM IBMX, 20°C		++		55		3.6
	Low Ca^{2+}/high Na^+, 20°C		++		0		2.9

+++ IFT observed, ++ IFT observed but more difficult to visualize than in *pf1* control, −− no IFT observed.
*Beads scored on 30–100 flagella at each time and condition.
‡30 flagella measured for each time and condition.

(Table I), indicating that flagellar resorption in itself does not cause the loss of IFT and bead movement. This result, therefore, implies that in *pf1 fla10* cells at 32°C the loss of IFT and bead movement, which is concomitant with a decrease in flagellar length, is not a *consequence* of the temperature-induced flagellar shortening, and the absence of IFT in itself may be the *cause* of temperature-induced flagellar shortening.

Relationship of IFT Particles to Rafts

Because we observed by video-enhanced DIC microscopy a decrease in the number of IFT particles (Fig. 1 *a*) in *pf1 fla10* flagella at 32°C (Table I), we asked whether the disappearance of IFT correlated with a loss of the electron dense complexes or "rafts" beneath the flagellar membrane (Fig. 1, *b–d*). We previously hypothesized (Kozminski et al., 1993*b*) that the IFT particles observed by light microscopy were the rafts observed by electron microscopy. *fla10*, *pf1 fla10*, and *pf1* cells were incubated at both the permissive and restrictive temperatures, fixed, and thin-sectioned for a quantitative EM analysis of the rafts.

After shifting *fla10* or *pf1 fla10* cells from 20 to 32°C for 90 min (i.e., conditions that inhibit IFT and bead movement), the ultrastructure of the resorbing flagella remained normal, except that the average number of rafts (Fig. 1, *b–d*) between the axonemal outer doublet microtubules and flagellar membrane decreased by 60–70% per transverse section (Table II). The slight decrease observed with *pf1* control cells under the same conditions (Table II) was not statistically significant (*t*-test). In addition, no decrease in the average number of rafts per section was observed when flagellar resorption was induced at 20°C, as a control, with IBMX or low calcium/high sodium medium (Table II). Because we also know that bead movement is abolished in low calcium/high sodium medium (Table I), this latter result did not support a correlation between the presence of rafts and bead movement, though it still remains possible that rafts move beads and that under these particular conditions bead movement is experimentally uncoupled from the rafts. In all experiments, however, the presence and absence of rafts did correlate with the presence and absence of IFT particles, suggesting that the particles observed moving by DIC microscopy are indeed the rafts observed by electron microscopy.

The relationship between IFT particles and rafts was further examined by correlating the position of IFT particles and rafts in light and electron micrographs of the same cell. When glutaraldehyde was perfused into specimen chambers, moving IFT particles stopped abruptly and remained fixed in place; the largest particles appeared, as in single video frame images of unfixed cells (Fig. 1 *a*), as bumps beneath the flagellar membrane. Although these cells, which were video-taped during fixation, would have been ideal for correlative electron microscopy, we found that fixed cells adhered poorly to the glass coverslips required for DIC microscopy and thus could not be permanently fixed in place during the embedding process. Therefore, cells were fixed, flat-embedded in resin, and then observed by video-enhanced DIC microscopy for fixed IFT particles (Fig. 2 *a*) before thin-sectioning. Although the resin decreased resolution, the flagellar topology of these flat-embedded cells when viewed by video-enhanced DIC microscopy was indistinguishable from that of fixed unembedded cells. Fig. 2 *a* shows three prominent IFT particles (labeled *1*, *2*, and *3*) in a flagellum of a flat-embedded cell. When serial thin sections of the same cell were examined by electron microscopy (Fig. 2, *b–d*) and aligned with the video-enhanced DIC image shown in Fig. 2 *a*, the positions of the three prominent IFT particles corresponded to the positions of rafts (labeled *1*, *2*, and *3*, respectively) beneath the flagellar membrane. This alignment indicates that the rafts observed by electron microscopy are the IFT particles observed by video-enhanced DIC microscopy.

FLA10 Antibody

Multiple klps have been identified in the flagella of *Chlamydomonas* by molecular and immunological methods (reviewed in Bernstein and Rosenbaum, 1994). On im-

Table II. Electron Microscopy Observations of Rafts in fla10 Cells

Cell line	Mean number of rafts/ transverse flagellar section (*n*) 0 min		90 min		Condition
pf1	1.1	(79)	0.90	(50)	32°C
fla10	0.68	(53)	0.28	(50)	32°C
pf1 fla10	1.2	(50)	0.42	(50)	32°C
pf1 fla10	0.84	(50)	1.1	(38)	0.5 mM IBMX, 20°C
pf1 fla10	0.76	(107)	0.87	(30)	Low Ca^{2+}/high Na^+, 20°C

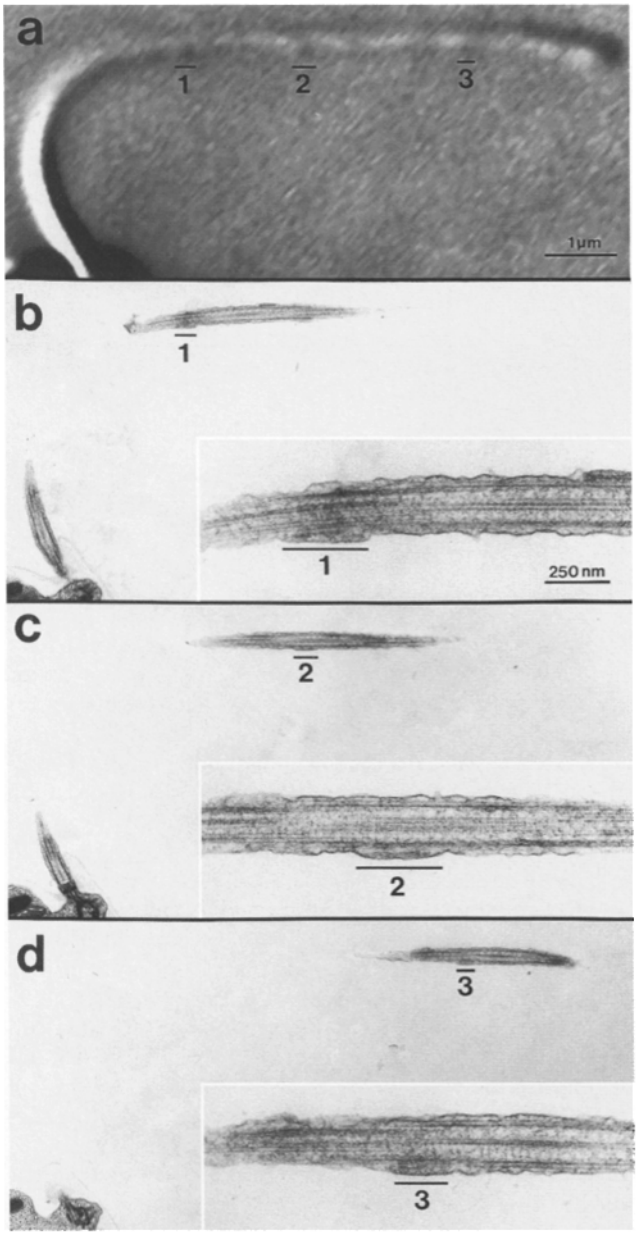

Figure 2. A single flat-embedded *Chlamydomonas* cell visualized with light and electron microscopy. One flagellum is shown as the region of interest. A portion of the cell body is visible in the lower left of each micrograph. (*a*) Video-enhanced DIC image: the most obvious IFT particles are numbered 1, 2, and 3. (*b–d*) Thin-sections 4 (*b*), 5 (*c*), and 8 (*d*) from a series through the cell shown in *a*. The numbered IFT particles in (*a*) correspond with electron-dense rafts in (*b–d*); insets show the rafts at higher magnification. The light micrograph (*a*) and low magnification electron micrographs (*b–d*) are printed at exactly the same magnification and mounted in the same orientation.

munoblots of axonemes, four klps (125, 110, 97, and 90 kD) were recognized by the affinity-purified LAGSE antibody (Fig. 3, lane *1*; Fox et al., 1994; Johnson et al., 1994), which was raised against a peptide in the conserved klp motor domain (Sawin et al., 1992). Flagellar polypeptides migrating outside the 90–125-kD range were also recognized by the LAGSE antibody, but the identities of these polypeptides remain unknown.

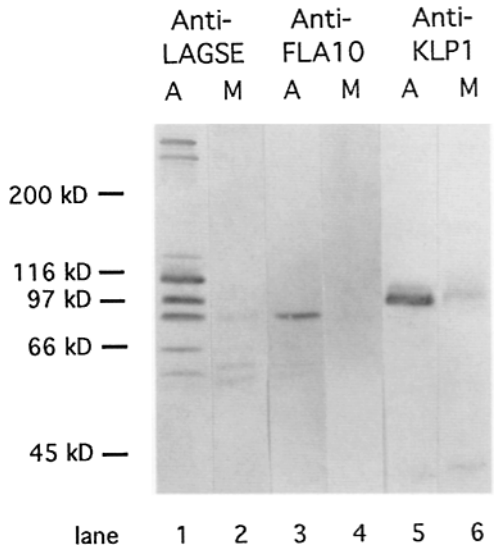

Figure 3. Immunoblots of flagellar fractions probed with anti-klp antibodies. Wild-type (*21gr*) axonemes (*A*) and the membrane + matrix fraction (*M*) were loaded stoichiometrically. Axonemal lanes contain 15 μg of total protein.

To obtain a probe that specifically recognizes FLA10, we raised a polyclonal antibody against a bacterially expressed, nonconserved region of the FLA10 tail (see Material and Methods). On immunoblots, the affinity-purified FLA10 antibody recognized a single polypeptide of ~90 kD in the axonemal fraction of detergent-extracted *Chlamydomonas* flagella (Fig. 3, lane *3*). This 90–kD polypeptide comigrated with an axonemal polypeptide recognized by the LAGSE antibody (Fig. 3, lane *1*); both polypeptides were extractable with 10 mM MgATP (data not shown) and were clearly distinguishable from KLP1 (Fig. 3, lane *5*), a 97-kD central pair-associated klp (Bernstein et al., 1994) that was also extractable with 10 mM MgATP (data not shown). Like the ATP-extractable ~90-kD axonemal polypeptide recognized by 14-02, an antibody raised against a smaller portion of the nonconserved tail region of FLA10 (Walther et al., 1994), the 90-kD ATP-extractable axonemal polypeptide recognized by the FLA10 antibody is also reduced in the flagella of *fla10-1* cells in comparison to control cells (see Fig. 4 *b*, *bottom*; Fig. 7 in Walther et al., 1994), strongly suggesting that the FLA10 antibody recognizes the same polypeptide as 14-02.

FLA 10 Levels In The Flagella During Temperature-Induced Flagellar Resorption

The simplest explanation for the temperature-sensitive phenotype of *fla10* cells is the destabilization of FLA10 at elevated temperatures, leading to the inactivation and/or rapid degradation of FLA10. Among the *Chlamydomonas* strains temperature-sensitive for flagellar assembly and stability, the sensitivity of a mutant polypeptide to temperature can vary depending upon its location within the cell (Huang et al., 1977; Shiota et al., 1979). In a series of experiments that used flagellar length as an indicator of FLA10 function, FLA10 appeared to be irreversibly destabilized by elevated temperatures in both the flagella and the cell body of *fla10* cells (data not shown). To test for

temperature-induced destabilization of FLA10 in flagella, we took advantage of the fact that *Chlamydomonas* cells can reuse flagellar polypeptides, which have been resorbed into the cell body, for the assembly of new flagella (Coyne and Rosenbaum, 1970; Lefebvre et al., 1978). Gametes, which have a very small precursor pool (Lefebvre et al., 1978), were induced to resorb their flagella (low calcium/high sodium medium) at 32°C in the presence of cycloheximide, an inhibitor of protein synthesis. When shifted down to 20°C, *fla10* gametes, unlike wild-type gametes, could not regenerate their flagella utilizing the precursor pool of 32°C-treated polypeptides obtained from flagella resorbed at 32°C. These results indicated that FLA10 was irreversibly destabilized in the flagella of the *fla10* mutant and that the removal of cycloheximide (i.e., new protein synthesis) was required for the assembly of new flagella. FLA10 was also shown to be irreversibly destabilized by elevated temperatures when it is located in the cell body. It is known that when vegetative wild-type (*21gr*) cells are deflagellated in the presence of cycloheximide, half-length flagella can be assembled from a pool of precursors located within the cell body (Rosenbaum et al., 1969); this is also true for *fla10* cells at 20°C. However, when *fla10* cells were incubated for 45 min at 32°C in 10 μg/ml cycloheximide and then deflagellated, no flagellar regeneration occurred, even after cells were shifted down to 20°C (see also, Dutcher, 1986).

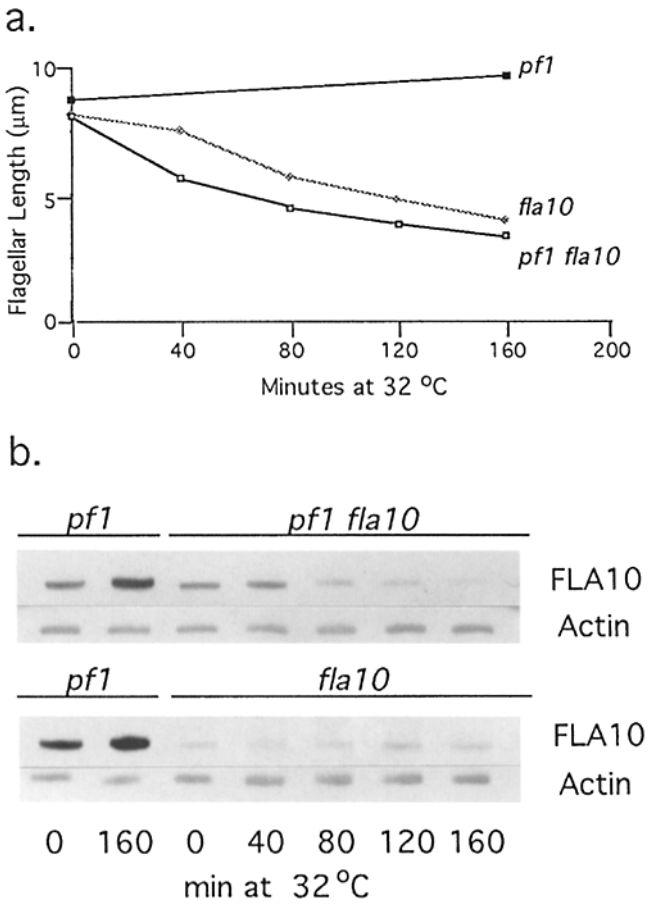

Figure 4. (*a*) Time course showing the mean flagellar length of cells in 5% sucrose in 10 mM Hepes (pH 7.4) at varying periods of time after the shift from 20 to 32°C. Flagella were isolated from *pf1* (*solid squares*), *fla10* (*solid diamonds*), and *pf1 fla10* (*open squares*) cells at each time point. In contrast to the cells bearing the *fla10* allele, the flagella of *pf1* control cells displayed an increase in FLA10 levels after 160 min at 32°C (Fig. 4 *b*, both panels) and, in 5% sucrose in 10 mM Hepes, no decrease in flagellar length. It is not known why *pf1* cells still maintained a normal flagellar length in 5% sucrose at 32°C at 160 min after the temperature shift; whereas, in culture medium under the same conditions, *pf1* cells begin to resorb their flagella. (*b*) Immunoblots of the flagella isolated at each of the time points shown in *a* probed with FLA10 antibody and reprobed with *Volvox* actin antibody to ensure equivalent sample loads. Each lane contains 15 μg of total flagellar protein.

The antibody specific for FLA10 enabled us to monitor, on immunoblots, the amount of FLA10 in flagella isolated from cells maintained at 20 and 32°C for varying periods of time. An actin antibody was used to reprobe the same immunoblots to demonstrate equivalent sample loads (Fig. 4 *b*). FLA10 levels were considerably reduced, even at the permissive temperature, in the flagella of *fla10* cells as compared to *pf1* cells (Fig. 4 *b*, *bottom*, compare 0 time points). The cause of this reduction in *fla10* cells could be due to a decreased level of FLA10 synthesis, the rapid degradation of FLA10, or the failure of FLA10 to enter the flagellum. Because the flagella of *fla10* cells appeared structurally (i.e., length and rafts; see Fig. 4 *a* and Table II, respectively) and functionally (i.e., beating) intact at 20°C, albeit with a greatly reduced amount of FLA10 in comparison to *pf1* control cells, it may be that more FLA10 per flagellum is necessary to maintain flagellar structure and function at elevated temperatures. This hypothesis is supported by the observations made when *pf1* and *fla10* cultures were shifted from 20 to 32°C: for the period of the experiment, the flagella of *pf1* cells maintained a constant length (Fig. 4 *a*) and exhibited an increased amount of FLA10 (Fig. 4 *b*); whereas, the flagella of *fla10* cells lost flagellar length (Fig. 4 *a*) and maintained a very low level of FLA10 (Fig. 4 *b*, *bottom*). The flagella of *pf1 fla10* cells, however, produced different results. At time 0, FLA10 levels in the flagella of *pf1 fla10* cells approximated control levels (compare 0 time points of *pf1* and *pf1 fla10*) and then declined 40-80 min post-temperature shift (Fig. 4 *b*, *top*). Although there is a difference in the FLA10 levels of *fla10* and *pf1 fla10* cells at 0 time, which may be due to the *pf1* background, it is important to note that a failure to maintain or increase FLA10 levels in *pf1 fla10* cells at 32°C, as in *fla10* cells, is accompanied by a concomitant loss of flagellar structure (i.e., length and rafts; see Fig. 4 *a* and Table II, respectively) and function (i.e., IFT and bead movement; see Table I). In both of the above examples, cells bearing the *fla10* allele neither had nor maintained sufficient FLA10 levels at 32°C to ensure normal flagellar structure and function. Therefore, the flagella of cells bearing the *fla10* allele may be defective at elevated temperatures not solely because FLA10 is destabilized, but because the elevated temperatures may increase the requirement for FLA10, a requirement that cannot be met in *fla10* strains.

Immunolocalization of FLA10

The temperature-shift, video-enhanced DIC microscopy

data (Table I) indicated that FLA10 is necessary for two flagellar membrane-associated motilities, IFT and bead movement. To first determine whether any flagellar klp is situated in proximity to the flagellar membrane, and thus in a position to drive IFT and bead movement, immunogold labeling of thin-sections was performed with the LAGSE antibody, which should recognize any klp bearing the conserved LAGSE domain including FLA10. In transverse sections, 30% of the labeling (n = 249 gold particles) was found in the region between the axonemal outer doublet microtubules and the flagellar membrane (Fig. 5, *a–d*). On occasion, the LAGSE antibody also labeled the rafts between the outer doublet microtubules and flagellar membrane (Fig. 5 *c*, *arrow*), although the method of sample preparation for immunogold labeling precluded the routine visualization of the rafts. In addition, the LAGSE antibody labeled the central pair microtubules (Fig. 5, *a* and *d*), reflecting, most likely, labeling of the 97- (KLP1; Bernstein et al., 1994) and 110-kD klps (Johnson et al., 1994) that were previously localized to the central pair microtubules.

The affinity-purified FLA10 antibody provided a FLA10-specific probe that *only* labeled the region between the axonemal outer doublet microtubules and the flagellar membrane (Fig. 5, *e–h*); label was never found on the central pair microtubules or anywhere else within the core of the axoneme. No flagellar labeling was observed on control sections when the primary antibody was omitted or, in the case of the FLA10 antibody, when the antibody was blocked with the bacterially-expressed FLA10 peptide before incubation with the sections. These data, therefore,

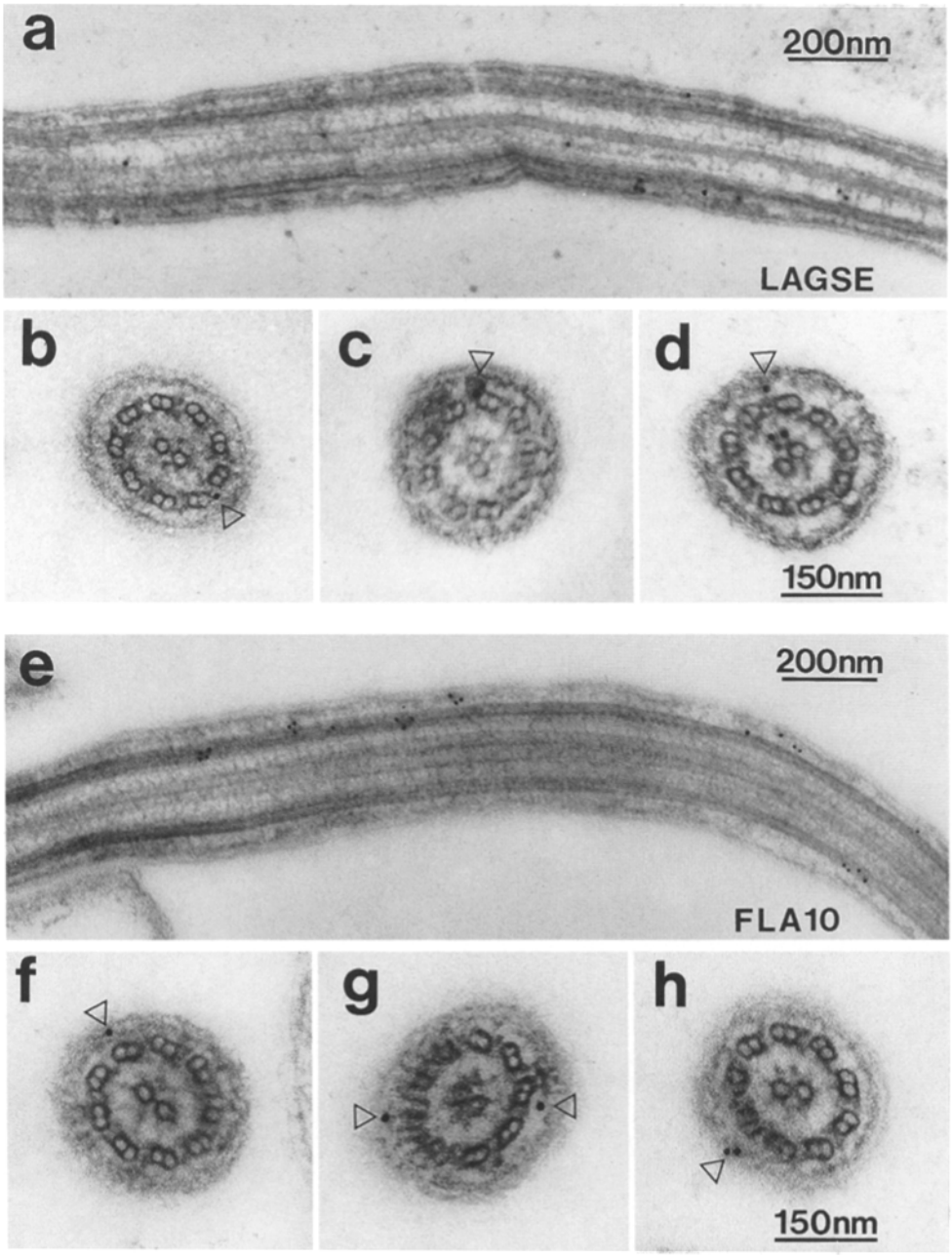

Figure 5. EM immunogold localization of FLA10 in wild-type (*21gr*) flagella using the LAGSE (*a–d*) or FLA10 antibody (*e–h*). Note that both antibodies labeled the region between the flagellar membrane and outer doublet microtubules shown in longitudinal (*a* and *e*) and transverse sections (*b–d* and *f–h*, *arrowheads*). The FLA10 antibody labeled the region beneath the membrane specifically; whereas, the LASGE antibody also labeled the klps associated with the central pair microtubules (*a* and *d*). Gold particles are 12 nm in diameter.

indicate that FLA10 is situated in proximity to the flagellar membrane and in a position to drive motilities associated with the flagellar membrane.

Discussion

By using a temperature-sensitive allele of the *Chlamydomonas FLA10* gene, we have determined that a flagellar klp is necessary for two motilities that occur in association with the flagellar membrane. Both motilities, IFT and bead movement, were arrested at the restrictive temperature in *pf1* (paralyzed-flagella) cells containing the *fla10* allele. Additionally, we have correlated the presence and position of the IFT particles observed by light microscopy with the presence and position of the rafts observed beneath the flagellar membrane by electron microscopy. A role for FLA10 in IFT and bead movement is also strongly supported by the immunolocalization of FLA10 to the region between the axonemal outer doublet microtubules and the flagellar membrane. Before this study, all of the flagellar klps examined cytologically were localized to the central pair apparatus (Bernstein et al., 1994; Johnson et al., 1994). Of the five or six known flagellar klps, FLA10 is the only klp situated within the flagellum that could drive motility on or beneath the flagellar membrane.

Number of Flagellar Klps

The immunoblot data in this report combined with previous reports show that there are at least five flagellar klps in *Chlamydomonas*. On our gradient gels, the 97- and 90-kD polypeptides recognized by the LAGSE antibody comigrated with the polypeptides recognized by the KLP1 and FLA10 antibodies, respectively. We propose that the polypeptide observed by Fox et al. at 97 kD (Fox et al., 1994) is FLA10 because both FLA10 and the 97-kD polypeptide of Fox et al. are extractable from axonemes with ATP (Fox et al., 1994; Walther et al., 1994), are present in mutants lacking the central pair microtubules (Fox et al., 1994; Johnson et al., 1994; Walther et al., 1994), and are recognized by the pan-klp LAGSE and HIPYR antibodies (Fox et al., 1994; Johnson et al., 1994). The five known flagellar klps in *Chlamydomonas*, therefore, are 125 (unlocalized), 110 (central pair-associated), 110 (central pair-associated), 97 (KLP1; central pair-associated), and 90 kD (FLA10; outer doublet-associated beneath the flagellar membrane).

Relationship of IFT Particles to Rafts

Shifting *pf1 fla10* cells to 32°C resulted both in a loss of the IFT particles observed by light microscopy and a significant reduction in the number of rafts between the flagellar membrane and axoneme as observed by electron microscopy. After 90 min at 32°C, no IFT particles were observed with video-enhanced DIC microscopy, but one-third of the rafts remained. A possible explanation for these remaining rafts is the difference in resolution afforded by light and electron microscopy. In comparison to the visibility of the IFT particles in the light microscope, rafts are relatively easy to find and score in thin-sections. Nevertheless, the experiment correlating the spatial relationship between the rafts and IFT particles (Fig. 2) strongly suggests that the prominent IFT particles in the light microscope are the rafts seen beneath the flagellar membrane by electron microscopy.

Although bead movement ceased and the number of rafts decreased at 32°C in the flagella of cells bearing the *fla10* allele, correlative light and electron microscopy data also showed that it is possible to completely arrest bead movement with low calcium/high sodium medium without reducing the number of rafts. This observation is consistent with the possibility that beads may be not carried along the length of the flagellum by the rafts/IFT particles. Bead movement on the reticulopodia of *Allogromia* and the axopodia of *Echinosphaerium*, likewise, has also been shown to be independent of the movement of large complexes beneath the plasma membrane (Bowser and Bloodgood, 1984). However, it remains possible that beads are moved by rafts/IFT particles. Under particular medium conditions, such as low calcium/high sodium, bead movement may stop because the beads uncouple from the rafts/IFT particles. Along with our earlier observations (Kozminski et al., 1993*b*), however, that beads move independently of IFT particles and display different rates of movement (discussed further below), the arrest of bead movement without a concomitant loss of rafts more strongly suggests that IFT and bead movement are two different motilities.

FLA10 Function

Although a temperature-sensitive mutant allowed us to demonstrate that FLA10 is necessary for IFT and bead movement, we cannot, at present, determine the direct contribution of FLA10 to each of these motilities. Because IFT, but not bead movement, is reduced (i.e., number of IFT particles) at the permissive temperature in *pf1 fla10* cells, it appears that IFT has a greater dependence on normal FLA10 activity than bead movement. At the restrictive temperature, both motilities were affected in the *fla10* mutant. It remains to be shown, however, whether FLA10 directly participates in one or both motilities, if one motility is dependent upon the other, or if FLA10 is involved in an undefined motility that acts upstream of IFT and bead movement. Based on the rates of movement, it seems unlikely that both IFT and bead movement are driven by the same motor. IFT proceeds at approximately 2 μm/s toward the flagellar tip and 3.5 μm/s toward the flagellar base (Kozminski et al., 1993*b*), whereas bead movement occurs at ~1.1–1.7 μm/s in both directions (Bloodgood, 1977; Kozminski et al., 1993*b*). In addition, IFT was observed to proceed normally in mutants in which bead movement does not occur or when bead movement is experimentally arrested (Kozminski et al., 1993*b*). Considering these observations and the fact that IFT is difficult to arrest without inducing deflagellation or cell death (unpublished observations), it is possible that IFT is at the top of a hierarchy of flagellar motilities. IFT, therefore, may be central to the maintenance of flagellar integrity. Disruption of a motor involved in IFT would have pleiotropic effects, resulting not only in the loss of flagellar length and bead movement, but that of other flagellar motilities as well (e.g., flagellar beating).

Because the motor domain of FLA10 is NH_2-terminal (Walther et al., 1994), like that of microtubule plus end-directed motors (Goodson et al., 1994), FLA 10 would be

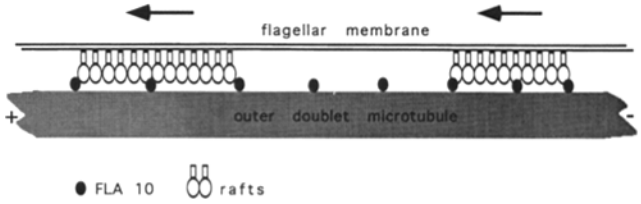

Figure 6. Model illustrating the involvement of FLA10 with IFT directed toward the flagellar tip. The IFT particles observed by light microscopy are the rafts observed beneath the flagellar membrane by electron microscopy. FLA10 is distributed along the length of the outer doublet microtubules, interacting with the microtubule by its motor domain and with the rafts by its tail domain.

a suitable motor for transport of materials to the flagellar tip, where the plus ends of all the axonemal microtubules are located (Allen and Borisy, 1974; Binder et al., 1975). Considering that FLA10 appears to be involved with IFT and that IFT particles correlate with rafts beneath the flagellar membrane, FLA10 could be modeled as the motor moving the rafts along the length of the flagellum to the flagellar tip (Fig. 6). FLA10 is certainly in a correct position within the flagellum to drive IFT; that is, FLA10 is localized between the flagellar membrane and the outer doublet microtubules. In a few thin-sections, FLA10 is localized by immunogold labeling to rafts; however, the staining method used in conjunction with the immunogold labeling technique precludes the routine visualization of rafts, thus preventing a conclusive localization of FLA10 to rafts. A potential problem with the proposed model arises from the observation that IFT ceased in both directions along the length of the flagella when *fla10* cells were shifted to 32°C. That is, microtubule minus end-directed motility ceased with the temperature-induced perturbation of a microtubule plus end-directed motor. Analogous results, however, can be found in axons, where all the microtubule plus ends are, as in the flagellum, distal to the cell body (Burton and Paige, 1981; Heidemann et al., 1981). In extruded axoplasm, perfusion of anti-kinesin antibodies not only blocked anterograde transport, but retrograde transport as well (Brady et al., 1990). As with axonal transport (Grafstein and Forman, 1980; Vallee et al., 1989), retrograde motility in the flagellum may depend upon anterograde motility for transport to the flagellar tip of the retrograde motor and/or retrograde "cargo" container. At present, the composition of the rafts, cargo, and retrograde motor remains unknown, though we speculate that the retrograde motor may be either a cytoplasmic dynein or a second kinesin with a minus end-directed motor.

Future Directions

The use of a temperature sensitive mutant in this study not only helped us to correlate our light and electron microscopy data, but, more importantly, demonstrated the necessity of a flagellar klp for IFT and bead movement. We have found that IFT and bead movement also arrested in *fla1* and *fla3* cells when those cells were shifted to 32°C for 90 min (unpublished observation). Because all the *FLA* loci were identified in mutant screens by virtue of the same phenotype (i.e., flagellar instability at 32°C) (Huang et al., 1977; Adams et al., 1982), it is not unusual to expect that the *FLA1* and *FLA3* genes also encode products required for IFT and bead movement. These gene products may be in a biochemical pathway that modulates motor function or in a complex with FLA10. Considering the previous analogy between IFT and axonal transport, the latter prospect is exciting, especially in view of the homology between FLA10 (Walther et al., 1994) and KIF3A, a plus end-directed axonal kinesin from mouse that, like its homologue, KRP85/95 from sea urchin (Cole et al., 1993), forms heterotrimeric complexes (Kondo et al., 1994).

The authors would like to thank M. Bernstein, D. Diener, and W. Mages for critical comments and discussion. We also thank M. Bernstein for his assistance with cloning the FLA10 tail sequence, P. Forscher for helpful discussions and the kind use of his microscope, as well as S. Limbach and G. Borisy for sharing their ideas on thermal microscope chambers.

Parts of this work were completed by K. G. Kozminski in partial fulfillment of the requirements for the degree of Doctor of Philosophy (Yale University) and was supported by National Institutes of Health grant GM14642 and National Science Foundation grant 45147 to J. L. Rosenbaum.

Received for publication 21 July 1995 and in revised form 8 September 1995.

References

Adams, G. M. W., B. Huang, and D. J. L. Luck. 1982. Temperature-sensitive, assembly-defective flagella mutants of *Chlamydomonas reinhardtii*. *Genetics.* 100:579–586.

Allen, C., and G. G. Borisy. 1974. Structural polarity and directional growth of microtubules of Chlamydomonas flagella. *J. Mol. Biol.* 90:381–402.

Bernstein, M., and J. L. Rosenbaum. 1994. Kinesin-like proteins in the flagella of *Chlamydomonas*. *Trends Cell Biol.* 4:236–240.

Bernstein, M., P. L. Beech, S. G. Katz, and J. L. Rosenbaum. 1994. A new kinesin-like protein (Klp1) localized to a single microtubule of the *Chlamydomonas* flagellum. *J. Cell Biol.* 125:1313–1326.

Binder, L. I., W. L. Dentler, and J. L. Rosenbaum. 1975. Assembly of chick brain tubulin onto flagellar microtubules from *Chlamydomonas* and sea urchin sperm. *Proc. Natl. Acad. Sci. USA.* 72:1122–1126.

Bloodgood, R. A. 1977. Motility occurring in association with the surface of the *Chlamydomonas* flagellum. *J. Cell Biol.* 75:983–989.

Bloodgood, R. A. 1981. Flagella-dependent gliding motility in *Chlamydomonas*. *Protoplasma.* 106:183–192.

Bloodgood, R. A. 1990. Gliding motility and flagellar glycoprotein dynamics in *Chlamydomonas*. *In* Ciliary and Flagellar Membranes. R. A. Bloodgood, editor. Plenum Press, NY. 91–128.

Bloodgood, R. A. 1992. Directed movements of ciliary and flagellar membrane components: a review. *Biol. Cell.* 76:291–302.

Bloodgood, R. A. 1995. Flagellar surface motility: gliding and microsphere movements. *In* Cilia and Flagella. W. L. Dentler and G. B. Witman, editors. Academic Press, NY. 273–279.

Bloodgood, R. A., E. M. Leffler, and A. T. Bojczuk. 1979. Reversible inhibition of *Chlamydomonas* flagellar surface motility. *J. Cell Biol.* 82:664–674.

Bowser, S. S., and R. A. Bloodgood. 1984. Evidence against surf-riding as a general mechanism for surface motility. *Cell Motil.* 4:305–314.

Brady, S. T., K. K. Pfister, and G. S. Bloom. 1990. A monoclonal antibody against kinesin inhibits both anterograde and retrograde fast axonal transport in squid axoplasm. *Proc. Natl. Acad. Sci. USA.* 87:1061–1065.

Burton, P. R., and J. L. Paige. 1981. Polarity of axoplasmic microtubules in the olfactory nerve of the frog. *Proc. Natl. Acad. Sci. USA.* 78:3269–3273.

Cole, D. G., S. W. Chinn, K. P. Wedaman, K. Hall, T. Vuong, and J. M. Scholey. 1993. Novel heterotrimeric kinesin-related protein purified from sea urchin eggs. *Nature (Lond.).* 366:268–270.

Coyne, B., and J. L. Rosenbaum. 1970. Flagellar elongation and shortening in *Chlamydomonas* II. Reutilization of flagellar proteins. *J. Cell Biol.* 47:777–781.

Curry, A. M., B. D. Williams and J. L. Rosenbaum. 1992. Sequence analysis reveals homology between two proteins of the flagellar radial spoke. *Mol. Cell. Biol.* 12:3967–3977.

Dutcher, S. K. 1986. Genetic properties of linkage group XIX in *Chlamydomonas reinhardtii*. *In* Extrachromosomal Elements in Lower Eukaryotes. R. B. Wickner, A. Hinnebusch, A. M. Lambowitz, I. C. Gunsalus, and A. Hollaender, editors. Plenum Press, NY. 303–325.

Dutcher, S. K. 1989. Genetic analysis of microtubule organizing centers. *In* Cell Movement. F. D. Warner and J. R. McIntosh, editors. Alan Liss, Inc., NY.

83–94.
Dutcher, S. K. 1995. Genetic nomenclature guide. *Trends Genet.* 11(Suppl.):18–19.
Fox, L. A., K. E. Sawin, and W. S. Sale. 1992. Evidence for kinesin-related proteins in eukaryotic flagella. *Mol. Biol. Cell.* 3:367.
Fox, L. A., K. E. Sawin, and W. S. Sale. 1994. Kinesin-related proteins in eukaryotic flagella. *J. Cell Sci.* 107:1545–1550.
Goodson, H. V., S. J. Kang, and S. A. Endow. 1994. Molecular phylogeny of the kinesin family of microtubule motor proteins. *J. Cell Sci.* 107:1875–1884.
Grafstein, B., and D. S. Forman. 1980. Intracellular transport in neurons. *Physiol. Rev.* 60:1167–1283.
Heidemann, S. R., J. M. Landers, and M. A. Hamborg. 1981. Polarity orientation of axonal microtubules. *J. Cell Biol.* 91:661–665.
Huang, B. P.-H. 1986. *Chlamydomonas reinhardtii:* a model system for the genetic analysis of flagellar structure and motility. *Intl. Rev. Cytol.* 99:181–215.
Huang, B., M. R. Rifkin, and D. J. L. Luck. 1977. Temperature-sensitive mutations affecting flagellar assembly and function of *Chlamydomonas reinhardtii. J. Cell Biol.* 72:67–85.
James, S. W. 1989. Genetic and molecular analysis of *Chlamydomonas reinhardtii* mutants resistant to anti-microtubule herbicides. University of Minnesota. Ph.D. Thesis.
Jarvik, J. W., and J. L. Rosenbaum. 1980. Oversized flagellar membrane protein in paralyzed mutants of *Chlamydomonas reinhardtii. J. Cell Biol.* 85:258–272.
Johnson, K. A., M. A. Haas, and J. L. Rosenbaum. 1994. Localization of a kinesin-related protein to the central pair apparatus of the *Chlamydomonas reinhardtii* flagellum. *J. Cell Sci.* 107:1551–1556.
Kondo, S., R. Sato-Yoshitake, Y. Hoda, H. Aizawa, T. Nakata, Y. Matsuura, and N. Hirokawa. 1994. KIF3A is a new microtubule-based anterograde motor in the nerve axon. *J. Cell Biol.* 125:1095–1107.
Kozminski, K. G. 1995*a*. Beat-independent flagellar motilities in *Chlamydomonas* and an analysis of the function of α-tubulin acetylation. Yale University. Ph.D. Thesis. 151 pp.
Kozminski, K. G. 1995*b*. High-resolution imaging of flagella. *In* Cilia and Flagella. W. L. Dentler and G. B. Witman, editors. Academic Press, NY. 263–271.
Kozminski, K. G., K. A. Johnson, P. Forscher, and J. L. Rosenbaum. 1992. A new motility associated with the eukaryotic flagellum. *Mol. Biol. Cell.* 3:51.
Kozminski, K. G., D. R. Diener, and J. L. Rosenbaum. 1993*a*. High level expression of nonacetylatable α-tubulin in *Chlamydomonas reinhardtii. Cell Motil. Cytoskeleton.* 25:158–170.
Kozminski, K. G., K. A. Johnson, P. Forscher, and J. L. Rosenbaum. 1993*b*. A motility in the eukaryotic flagellum unrelated to flagellar beating. *Proc. Natl. Acad. Sci. USA.* 90:5519–5523.
Kozminski, K. G., P. Forscher, and J. L. Rosenbaum. 1995. Three non-beat flagellar motilities in *Chlamydomonas. Cell Motil. Cytoskeleton. (Video Supplement).* In Press.
Laemmli, U. K. 1970. Cleavage of structural proteins during the assembly of the head of bacteriophage T4. *Nature (Lond.).* 227:680–685.
Lefebvre, P. A., S. A. Nordstrom, J. E. Moulder, and J. L. Rosenbaum. 1978. Flagellar elongation and shortening in *Chlamydomonas* IV. Effects of flagellar detachment, regeneration, and resorption on the induction of flagellar protein synthesis. *J. Cell Biol.* 78:8–27.
Lefebvre, P. A., C. D. Silflow, E. D. Wieben, and J. L. Rosenbaum. 1980. Increased levels of mRNAs for tubulin and other flagellar proteins after amputation or shortening of Chlamydomonas flagella. *Cell.* 20:469–477.
Lewin, R. A. 1952. Studies on the flagella of algae. I. General observations of Chlamydomonas moewusii gerloff. *Biol. Bull. (Woods Hole).* 103:74–79.
Luck, D., G. Piperno, Z. Ramanis, and B. Huang. 1977. Flagellar mutants of *Chlamydomonas*: studies of radial spoke-defective strains by dikaryon and revertant analysis. *Proc. Natl. Acad. Sci. USA.* 74:3456–3460.
Lux, F. G. I., and S. K. Dutcher. 1991. Genetic interactions at the *FLA10* locus: suppressors and synthetic phenotypes that affect the cell cycle and flagellar function in *Chlamydomonas reinhardtii. Genetics.* 128:549–561.
Mesland, D. A. M., Hoffman, J. L., Caligor, E., and U. W. Goodenough. 1980. Flagellar tip activation stimulated by membrane adhesions in *Chlamydomonas* gametes. *J. Cell Biol.* 84:599–617.
Olmsted, J. B. 1981. Affinity purification of antibodies from diazotized paper blots of heterogeneous protein samples. *J. Biol. Chem.* 256:11955–11957.
Piperno, G., B. Huang, and D. J. L. Luck. 1977. Two-dimensional analysis of flagellar proteins from wild-type and paralyzed mutants of *Chlamydomonas reinhardtii. Proc. Natl. Acad. Sci. USA.* 74:1600–1604.
Reynolds, E. S. 1963. The use of lead citrate at high pH as an electron-opaque stain in electron microscopy. *J. Cell Biol.* 17:208–212.
Ringo, D. L. 1967. Flagellar motion and fine structure of the flagellar apparatus in *Chlamydomonas. J. Cell Biol.* 33:543–571.
Rosenbaum, J. L., J. E. Moulder, and D. L. Ringo. 1969. Flagellar elongation and shortening in *Chlamydomonas. J. Cell Biol.* 41:600–619.
Sager, R., and S. Granick. 1953. Nutritional studies with *Chlamydomonas reinhardtii. Ann. NY Acad. Sci.* 56:831–838.
Sawin, K. E., T. J. Mitchison, and L. G. Wordeman. 1992. Evidence for kinesin-related proteins in the mitotic apparatus using peptide antibodies. *J. Cell Sci.* 101:303–313.
Shiota, S., C. Sato, and M. Enomoto. 1979. Temperature-sensitive *Chlamydomonas* mutants manifesting flagellar regression at a restrictive temperature. *J. Protozool.* 26:232–234.
Snyder, M. 1989. The *SPA2* protein of yeast localizes to sites of cell growth. *J. Cell Biol.* 108:1419–1429.
Vallee, R. B., H. S. Shpetner, and B. M. Paschal. 1989. The role of dynein in retrograde axonal transport. *Trends Neurosci.* 12:66–70.
Walther, Z., M. Vashishtha, and J. L. Hall. 1994. The *Chlamydomonas FLA10* gene encodes a novel kinesin-homologous protein. *J. Cell Biol.* 126:175–188.
Witman, G. B. 1986. Isolation of *Chlamydomonas* flagella and flagellar axonemes. *Methods Enzymol.* 134:280–290.
Witman, G. B., K. Carlson, J. Berliner, and J. L. Rosenbaum. 1972. *Chlamydomonas* flagella I. Isolation and electrophoretic analysis of microtubules, matrix, membranes, and mastigonemes. *J. Cell Biol.* 54:507–539.